Synthesis and study of 2-amino- 7-bromofluorenes modified with nitroxides and their precursors as dual anti-amyloid and antioxidant active compounds

Tamás Kálai[a], **Jitka Petrlova**[b], **Mária Balog**[a], **Hnin Hnin Aung**[c], **John C. Voss**[b], and **Kálmán Hideg**[a,*]

[a]Institute of Organic and Medicinal Chemistry, University of Pécs, H-7624 Pécs, Szigeti st. 12. Pécs, Hungary

[b]Biochemistry & Molecular Medicine School of Medicine University, University of California Davis, One Shields Avenue, 4303 Tupper Hall Davis, CA 95616-8635, USA

[c]Division of Cardiovascular Medicine, Department of Internal Medicine, University of California Davis, Davis, CA 95616, USA

Abstract

A series of 2-aminofluorenes *N*-alkylated with nitroxides or their precursors were synthesized. The new compounds were tested on hydroxyl radical and peroxyl radical scavenging ability and inflammatory assay on the endothelial brain cells. In agreement with ROS scavenging ability the same compound 7-bromo-*N*–[(1-Oxyl-2,2,6,6-tetramethyl-1,2,3,6-tetrahydropyridine-4yl)methyl]-9*H*-fluoren-2-amine (**3b**) and its hydroxylamine salt (**3b/OH/HCl**) showed the anti-inflammatory property on the endothelial brain cells.

Keywords

Alzhemer's disease; antioxidants; free radicals; nitroxides; spin trapping

1. Introduction

Research on senile dementia and Alzhemer's disease (AD) covers an extremely broad range of scientific activities.[1] Formation of β-amyloid (Aβ) plaques in brain is the major contributing factor in the pathogenesis of AD. A β(25–35) is a highly toxic segment of amyloid Aβ-peptides which forms fibrillary aggregates. The etiology of AD is still not well understood; therefore neither prevention strategies nor long-term effective treatment modalities are available for this disease. Detection of Aβ plaques in the brain will be potentially useful in early diagnosis and monitoring progression of the disease. Identified imaging candidates include Congo red [2], benzothiazoles [3], dimethylaminofluorene [4] and stilbenes[5] just to mention a few examples. The high affinity of these compounds for assemblies of Aβ also provide clues for compounds that may serve as biophysical probes that can report the molecular events associated with AD. One class of biophysical probes is the sterically-hindered nitroxides, whose motion, chemical environment and spatial separation can be detected by electron paramagnetic resonance (EPR) spectroscopy. For example, EPR of nitroxides has evaluated the structure and dynamics of the Aβ peptide [6,

*Corresponding author: Kálmán Hideg, Institute of Organic and Medicinal Chemistry, University of Pécs, H-7624 Pécs, Szigeti st. 12. Pécs, Hungary, Phone:36-72-536-221, Fax: 36-72-536-219, kalman.hideg@aok.pte.hu.

7] and its interaction with membranes [8], as well as changes in membrane fluidity in individuals at risk for AD [9].

Attaching a nitroxide to structures that have high affinity for Aβ not only has potential for biophysical characterization of AD etiliogy, but also provides dual-action potential based on its unique ability to scavenge reactive oxygen species. As established in laboratory and clinical studies, reactive oxygen and nitrogen species represent major intermediary species in AD progression pathways that ultimately lead to neurodegeneration [10, 11]. In fact, accumulating evidence points to oxidative stress as the ultimate downstream component of Aβ-induced toxicity, involving a feedback loop that ultimately leads to neuronal self-digestion via mitochondrial dysfunction, increased Ca^{2+} levels, protein breakdown, free radical formation and lipid peroxidation [1, 2]. Cyclic nitroxides can be regarded as synthetic, multifunctional antioxidant molecules, owing their unique features to either their reduced forms, hydroxylamines or their oxidized forms oxoammonium cations [12]. It has been shown a decade ago [13] that nitroxides form superoxide dismutase mimetic oxoammonium cations, followed by reduction of the latter species with superoxide (eq. 1 and 2, Figure 1). Hydroxylamines can act as proton and electron donor molecules reducing any radical species (eq. 3.). Nitroxides are also capable of inhibiting ·OH formation by oxidizing Fe^{2+} to Fe^{3+} and hence preventing its participation in Fenton-reactions (eq. 4) [14]. The fully reduced form of the nitroxide – a sterically hindered amine – is easily oxidized to nitroxide by various ROS (eq. 5) [15]. This nitroxide is in an equilibrium with the hydroxylamine depending upon oxidative or reductive nature of its environment (eq. 6) [16].

While Aβ is known to modulate cascades leading to increased oxidative stress and apotosis, a direct participation of the peptide in generating ROS has also been identified. Dikalov et al. demonstrated that amyloid β peptides can enhance the metal catalyzed oxidation of hydroxilamines to nitroxides [17], and Butterfield et al. concluded that Aβ(25–35) peptide displays H_2O_2 like activity toward nitroxide spin probes [18]. Thus nitroxides targeted to the proximity of Aβ at cells may be especially useful.

As far as we know no study on Aβ aggregate specific ligands, such as fluorenes, with antioxidant tag (nitroxide or its precursor) has been reported yet. These compounds may be useful in diagnostics and on the other hand the therapeutic significance of new compounds as antioxidant (ROS scavenging) molecules are to prevent or slow the neurodegenerative processes. Reported herein are preliminary results of the structure-activity relationship, e.g ROS scavenging ability and anti-inflammatory properties of fluorenes modified on amino function with various nitroxides (five- or six-membered with or without substituents) or their reduced forms. Current treatments of AD include administration of nonsteroidal anti-inflammatory drugs, which inhibit the synthesis of prostaglandins reduce the rate of deterioration of cognitive functions in patients with advanced AD. Cholinergic drugs are also used in the treatment of AD [19]. For example, Aβ increases NMDA receptor activation, and one of the newer drugs for the treatment of AD (Memantine) targets NMDA receptors in order to block glutamate excitotoxicity. Among other pathways, over-stimulation of NMDA receptors activates phospholipase A, leading to elevated arachidonic acid levels, which in turn generates oxygen free radicals and further activation of phosholipases [3]. In summary, because Alzheimer's disease is a multi-factorial disease where oxidative stress represents a general pathogenic basis for the ultimate neuronal death, developing bi-functional compounds that both target the instigator of Alzheimer's as well the downstream consequences, represents a novel approach for treating this complex disease. Thus developing compounds that mitigate more than one process within the disease pathway are of particular interest.

1. Lin, M.T. and M.F. Beal, *Mitochondrial dysfunction and oxidative stress in neurodegenerative diseases.* Nature, 2006. **443**(7113): p. 787–95.

2. Lipton, S.A., *Paradigm shift in neuroprotection by NMDA receptor blockade: memantine and beyond.* Nat Rev Drug Discov, 2006. **5**(2): p. 160–70.

3. Farooqui, A.A., H.C. Yang, and L. Horrocks, *Involvement of phospholipase A2 in neurodegeneration.* Neurochem Int, 1997. **30**(6): p. 517–22.

2. Chemistry

The key reaction in synthesis of paramagnetic 2-amino-7-bromofluorenes is alkylation of compound **1** with equivalent amount allylic bromides (**2a-d**)[20–23] in the presence of K_2CO_3 in DMSO at 60 °C offered the monoalkylated products **3a-d** in 38–45% yield (Scheme 1). Hydroxylamine salt of compound **3b/OH/2HCl** was achieved by treatment of radical **3b** with ethanol saturated previously with HCl gas. Compound **3a** was methylated on aromatic nitrogen atom by treatment with paraformaldehyde and cyanoborohydride as a reducing agent in acetic acid to give compound **4** in 64% yield [4]. The sterically hindered amine derivative **5** was achieved by reduction of radical **4** with iron powder in acetic acid [24] (Scheme 1).

3. Results and discussion

Superoxide and hydroxyl radicals are the predominant reactive oxygen species that cause damage in cells. To evaluate the ability of our modified fluorenes to decrease the levels of produced hydroxyl radical, we used a hydroxyl radical antioxidant capacity (HORAC) assay, that uses a a reporter whose fluorescence is inversely proportional to the level of surving radical. We therefore measured the ability of each compound (at 0.2, 1 and 10 μM) to maintain indicator signal in the presence of hydroxyl radical. As shown in Figure 2, all of the fluorene compounds have a capability to scavenge hydroxyl radicals and all three concentrations were effective, although in general the efficiency of scavenging rises with the raising concentration of fluorene compounds. The most effective compounds are **3b, 3b/OH/HCl** and **5** (Figure 2). These findings are not unexpected, as the hydroxylamine salt compound **3b** has a lower redox potential and is more readily oxidized to nitroxide (see eq. 3 in Fig. 1.), compared to the corresponding five-membered, sterically hindered compounds. One of the five-membered compounds, the amine **5** readily oxidizes to stable nitroxide (eq. 5 of Fig. 1), which again is in good agreement with our previous results and assumptions [25]. In general, the hybrid of the fluorene with the nitroxide/nitroxide precursor provides superior hydroxyl scavenging activity compared to the base fluorene alone (KO-162; Scheme 2 and Fig. 2), where we have previously measured antioxidant activity [26]. The same is found when comparing the hybrids to a nitroxide alone (TEMPOL; Scheme 2 and Fig. 2), with the exception of the bromo-substituted **3c**. We also determined the efficiency of the compounds to scavenge superoxide radicals using the oxygen radical absorbance capacity (ORAC) assay using an indicator whose fluorescence is quenched by the radical. As shown in Figure 3, each of the of the fluorene compounds had some capability to scavenge peroxyl radicals at the 10 μM concentration. Among the compounds tested, sterically hindered amines, such as compound **3d** and compound **5** were the most efficient ones. Compounds **3b/OH/HCl** and **3c** also exhibited limited activity (Figure 3). Neither TEMPOL alone nor the base fluorene KO-162 exhibit significant scavenging of peroxyl radicals.

The levels of free radicals in solution can also be detected by EPR spectroscopy of spin trapping reagents. We used the 5-tert-butoxycarbonyl 5-methyl-1-pyrroline *N*-oxide (BMPO) spin trap due to its ability to form a more stable and distinctive adduct with

superoxide [27]. The EPR spectra of BMPO adduct with hydroxyl radicals (generated via iron(II)-sulfate/H_2O_2,) is shown in Figure 4 (grey). The spectrum of the fluorene compound **3b/OH/2HCl** alone is shown in dotted line. Upon generation of hydroxyl radicals, compound decreases by 61% the amount of BMPO-hydroxyl adduct (black line) compared to the sample without a fluorene compound addition (Figure 4). An efficient scavenging of the superoxide anion radical was observed by EPR (Figure 5). The superoxide anion (generated horseradish peroxidase/H_2O_2)–BMPO adduct (shown in grey) totally disappears by adding compound **3b/OH/2HCl,** while its triplet signal is increased shown in black. The spectrum of the fluorene compound **3b/OH/2HCl** alone is shown in dotted line (Figure 5). In agreement with results from ORAC assay we observe very strong peroxyl scavenging activity by compounds **3b, 3B/OH/2HCl, 3d** and **5** using EPR. Here again, fluorene compounds **3b/OH/2HCl** and **5** most significantly reduce the EPR signal of hydroxyl radicals (Table 1).

Inflammation has also been implicated in the etiology of AD [28]. We therefore also evaluated the new compounds for their ability to down-regulate markers of inflammation in a brain endothelial cell line. Figure 6 shows the anti-inflammatory activity of the compounds according to the expression of 3 marker genes as measured by RT-PCR. In the assay, genes encoding transcription factors, activating transcription factor 3 (ATF3) and inflammatory response genes interleukin 8 (IL-8) and prostaglandin-endoperoxide synthase 2 (PTGS2; also known as cyclooxygenase 2 (COX-2) were activated by TGRL lipolysis products in HBMVEC by 22.8, 1.8 and 3.1-fold, respectively. Compound **4** significantly suppresses lipolysis product-induced expression of ATF3 and COX-2 by 18.3 and 2.7 fold, respectively. Only a small, but insignificant supression of IL-8 expression is observed by compound **4**. ATF3 and especially IL-8 expression are also suppressed by compounds **3b/ OH/2HCl** and **3b**. Compounds **3a**, **3c**, **3d** and **5** further *increased* ATF3, IL-8 and COX-2 gene expressions.

4. Conclusion

A new series of 7-bromo-2-aminofluorene compounds were synthesized modified by nitroxides and their precursors. Among the new compounds compound **3b** and its hydroxylamine salt **3b/OH/HCl** has both ROS scavenge property (based on HORAC, ORAC and spin trapping assays) and anti-inflammatory property on the endothelial brain cells. The fluorene nitroxide precursor hybrid compounds exhibited better radical scavenging activity than TEMPOL or KO-162 (7-bromo-2-dimethylaminofluorene) compounds themselves. Four compounds increased ATF, IL-8 and COX-2 gene expressions, but three compounds (**3b, 3b/OH/HCl, 4**) have beneficial effects on inflammatory processes. The additions of the oanti-oxidant and anti-inflammatory activitites to fluorenes that target the toxic assembly of Aβ [X] and and its downstream activity provides a novel approach for treating AD. Further investigations with these compounds is under way.

X. Hong, H.S., et al., *Candidate anti-Abeta fluorene compounds selected from analogs of amyloid imaging agents.* Neurobiol Aging, 2008.

5. Experimental protocols

5. 1. Chemistry

Melting points were determined with a Boetius micro melting point apparatus and are uncorrected. Elemental analyses (C, H, N, S) were performed on Fisons EA 1110 CHNS elemental analyzer. Mass spectra were recorded on a Thermoquest Automass Multi and VG TRIO-2 instruments and in the EI mode. ^{1}H NMR spectra were recorded with Varian

UNITYINOVA 400 WB spectrometer. Chemical shifts are referenced to Me₄Si. Measurements were run at 298K probe temperature in CDCl₃ solution. ESR spectra were taken on Miniscope MS 200 in 10^{-4} M CHCl₃ solution and monoradicals gave triplett line.

Flash column chromatography was performed on Merck Kieselgel 60 (0.040-0.063 mm). Qualitative TLC was carried out on commercially available plates ($20 \times 20 \times 0.02$ cm) coated with Merck Kieselgel GF₂₅₄. TEMPOL and all other chemicals were purchased from Aldrich, compound **2a** [20], **2b** [21], **2c** [22], **2d** [23] and KO-162 [4] was prepared as described earlier.

5.1.1. Synthesis of compounds 3a, 3b, 3c, 3d; General procedure—A mixture of 7-bromo-2-aminofluorene **1** (520 mg, 2.0 mmol), K₂CO₃ (276 mg, 2.0 mmol) and allylic bromide **2a** or **2b** or **2c** or **2d** (2.0 mmol) in DMSO (10 mL) was stirred and heated at 60 °C till the consumption of starting materials (~6h). After cooling the mixture was poured onto water (50 mL), extracted with EtOAc (3 × 20 mL). The combined organic layer was washed with water (10 mL), the organic phase was dried (MgSO₄), filtered and evaporated. The residue was purified by flash column chromatography (hexane/EtOAc or CHCl₃/MeOH) to give the N-alkylated fluorenes in 38–45% yield.

5.1.1.1. 7-bromo-*N* –[(1-Oxyl-2,2,5,5-tetramethyl-2,5-dihydro-1H-pyrrol-3-yl)methyl]-9*H*-fluoren-2-amine Radical (3a): 130 mg, 40%, yellow solid, mp 177–180 °C, R_f: 0.32 (hexane-EtOAc, 2:1). MS (EI) *m/z* (%): 411/413 (M⁺, 17/17), 381/383 (15/15), 259/261 (100/100), 180 (82). Anal. Calcd. for C₂₂H₂₄BrN₂O C64.08, H5.87, N6.79; found: 64.00, H5.75, N 6.80.

5.1.1.2. 7-bromo-*N* –[(1-Oxyl-2,2,6,6-tetramethyl-1,2,3,6-hexahydropyridine-4-yl)methyl]-9*H*-fluoren-2-amine Radical (3b): 383 mg, 45%, deep yellow solid, mp 177–179 °C, R_f: 0.53 (hexane-EtOAc, 2:1). MS (EI) *m/z* (%): 425/427 (M⁺, 5/5), 395/397 (2/2), 272/274 (46/45), 259/261 (50/50), 154 (100). Anal. Calcd. for C₂₃H₂₆BrN₂O C64.79, H6.15, N6.57; found: 64.68, H6.02, N 6.39.

5.1.1.3. 7-bromo-*N* –[(1-Oxyl-4-bromo-2,2,5,5-tetramethyl-2,5-dihydro-1H-pyrrol-3-yl)methyl]-9*H*-fluoren-2-amine Radical (3c): 412 mg, 42%, yellow solid, mp 153–156 °C, R_f: 0.55 (hexane-EtOAc, 2:1). MS (EI) *m/z* (%): 489/491/493 (M⁺, 5/11/5), 459/461/463 (4/10/4), 272/274(100/100), 259/261 (48/48), 152 (49). Anal. Calcd. for C₂₂H₂₃Br₂N₂O C53.79, H4.72, N5.70; found: C53.66, H4.75, N5.54.

5.1.1.4. 7-bromo-*N* –[(1,2,2,5,5-pentamethyl-2,5-dihydro-1H-pyrrol-3-yl)methyl]-9*H*-fluoren-2-amine (3d): 312 mg, 38%, beige solid, mp 153–155 °C, R_f: 0.35 (CHCl₃-MeOH, 1:1). MS (EI) *m/z* (%): 410/412 (M⁺, 8/8), 395/397 (12/12), 272/274 (100/100), 124 (94). ¹H NMR (CD₃OD): δ: 1.22 (s, 6H), 1.35 (s, 6H), 2.45 (s, 3H), 3.76 (s, 2H), 3.85 (s, 2H) 5.59 (s, 1H), 6.66 d (J= 7.6 Hz), 6.81 (s, 1H), 7.39–7.55 (m, 4H). Anal. Calcd. for C₂₃H₂₇BrN₂ C67.15, H6.62, N6.81; found: C67.08, H6.58, N6.72.

5.1.2. 7-bromo-*N*-methyl-*N* –[(2,2,5,5-tetramethyl-2,5-dihydro-1H-pyrrol-3-yl)methyl]-9*H*-fluoren-2-amine Radical (4)—To a solution of compound **3a** (412 mg, 1.0 mmol) and paraformaldehyde (600 mg) in AcOH (5mL) NaBH₃CN (550 mg, 8.7 mmol) was added in 3 portions for 10 minutes under well ventilated hood. The mixture was stirred at rt. for 18h, then poured onto mixture of 40 g ice and 10% aq. NaOH (40 mL). After melting the ice the mixture was extracted with CH₂Cl₂ (2 × 20 mL), then the organic phase was dried (MgSO₄), PbO₂ (100 mg, 0.4 mmol) was added and O₂ was bubbled through the solution for 15 min. The solution was filtered, evaporated and the residue was purified by

flash column chromatography (hexane/EtOAc) to give the title compound as a yellow solid 273 mg (64%), mp 174–175 °C, R_f: 0.52 (hexane-EtOAc, 2:1). MS (EI) m/z (%): 425/427 (M$^+$, 20/20), 395/397 (7/7), 286/2288 (100/100), 43 (75). Anal. Calcd. for $C_{23}H_{26}BrN_2O$ C64.79, H6.15, N6.57; found: 64.74, H6.10, N 6.41.

5.1.3. 7-bromo-*N*-methyl-*N* –[(2,2,5,5-tetramethyl-2,5-dihydro-1H-pyrrol-3-yl)methyl]-9*H*-fluoren-2-amine (5)—To a solution of compound **4** (426 mg, 1.0 mmol) in glacial acetic acid (10 mL) Fe powder (560 mg, 10.0 mmol) was added and the mixture was warmed up to 70 °C until the reaction started and the mixture was stirred at rt. for 60 min. After diluting with water (30 mL) the solution was decanted from iron residue and in a 250 mL baker the solution was made alkaline (pH=9) by solid K_2CO_3 (intense foaming!). The mixture was extracted with $CHCl_3$/MeOH (9:1 mixture) (2 × 20 mL), the organic phase was dried ($MgSO_4$), filtered and evaporated. The residue was purified by flash column chromatography ($CHCl_3$:MeOH) to yield the title compound 193 mg (47%) as a beige solid, mp 160–162 °C, R_f: 0.39 ($CHCl_3$:MeOH, 2:1). MS (EI) m/z (%): 410/412 (M$^+$, 18/18), 395/397 (5/5), 286/288 (100/100), 122 (43). ^{1}H NMR (CD_3OD): δ: 1.22 (s, 6H), 1.38 (s, 6H), 3.03 (s, 3H), 3.78 (s, 2H), 3.99 (s, 2H) 5.27 (s, 1H), 6.71 dd (J= 8.6 Hz, J=2.2 Hz, 1 H), 6.89 (s, 1H), 7.36–7.55 (m, 4H). Anal. Calcd. for $C_{23}H_{27}BrN_2$ C67.15, H6.62, N6.81; found: 67.05, H6.50, N 6.69.

5.1.4. 7-Bromo-*N* –[(1-hydroxy-2,2,6,6-tetramethyl-1,2,3,6-hexahydropyridine-4-yl)methyl]-9*H*-fluoren-2-amine Radical Hydrochloride Salt (3b/OH/2HCl)—Compound **3b** (426 mg, 1. 0 mmol) was dissolved in 10 mL EtOH saturated previously with HCl gas and stirred at room temperature for 15 min, then solvent was evaporated off and the residue was crystallysed from acetone/Et_2O solution to give a pale yellow solid 352 mg (71 %), mp 202–205 °C. ^{1}H NMR (CD_3OD): δ: 1.37 (bs, 3H), 1.41 (bs, 3H), 1.48 (bs, 6H), 3.85 (s, 2H), 3.92 (s, 2H), 4.00 (s, 2H), 5.78 (s, 1H), 7.40 dd (J= 8.0 Hz, J=2.0 Hz, 1 H), 7.58 (s, 1H), 7.77–7.98 (m, 4H). Anal. Calcd. for $C_{23}H_{28}BrCl_2N_2O$ C 55.33, H 5.65, N 5.61; found: 55.20, H 5.80, N 5.40.

5.2. Biology assays

5.2.1. Antioxidant assays—For a determination of antioxidant activity of fluorene compounds Hydroxyl Radical Antioxidant Capacity (HORAC) assay (Cell Biolabs, INC., USA) was used. The samples were measured by Fluorescence microplate reader (Molecular Devices, SpectraMax M2) with a 485 nm excitation filter and 530 nm emission filter. The samples were prepared according a recommended protocol by the manufacture. For a determination of antioxidant activity of fluorene compounds toward peroxyl radicals we use The Oxygen Radical Antioxidant Capacity (ORAC) assay (Cell Biolabs, INC., USA). The samples were measured by Fluorescence microplate reader with a 480 nm excitation filter and 520 nm emission filter. The samples were prepared according a recommended protocol by the manufacture.

5.2.2 EPR measurements—Electron paramagnetic resonance measurements of BMPO spin traps were collected at room temperature with a JEOL X-band spectrometer fitted with a loop-gap resonator. For samples containing hydroxyl radicals, 1 μl of ammonium iron(II) sulfate, 1 μl of H_2O_2 (3%), 10 μl of BMPO (100 mM) and 88 μl of PBS pH 7.4. Nine microliters of the ROS mixture was then immediately combined with 1 μl of the fluorene compound (in a 2 mM stock), and approximately 5 μl of the samples was loaded into a sealed quartz capillary tube. For trapping in the presence of superoxide radicals, 2 μl of Horse Radish Peroxidase (10 mg/ml), 2 μl of H_2O_2 (3%), 2 μl of Na_3N, 2 μl of DTPA (100 mM), 46 ml of BMPO (100 mM) and 46 μl of PBS pH 7.4 were mixed and immediately combined with the fluorene compound (9 μl of the mixture and 1 μl of 2 mM fluorene). All

spectra were obtained by averaging two 2 minutes scans with a sweep width of 100 G at a microwave power of 3 mW and modulation amplitude optimized to the natural line width of the spin probe. All the spectra were recorded at room temperature.

5. 2. 3. Human TGRL isolation—This study was approved by the Human Subjects Review Committee at the University of California Davis. Postprandial blood samples were obtained 3.5 h after consumption of a moderately high fat meal, which corresponds to the peak elevation in plasma triglyceride concentrations. Triglyceride-rich lipoproteins (TGRL) were isolated from human plasma at d < 1.0063 g/mL by aspiration with a narrow-bore pipet followed by 18 h centrifugation at 40,000 rpm in a SW41 Ti swinging bucket rotor (Beckman Coulter, Sunnyvale, CA) held at 14°C within a Beckman L8-70M (Beckman) ultracentrifuge. The top fraction (TGRL) was collected and dialyzed in Spectrapor membrane tubing (mol wt cut off 3,500; Spectrum Medical Industries, Los Angeles, CA) at 4°C overnight against a saline solution containing 0.01%EDTA.

Lipoprotein lipase (LpL) was purchased from Sigma (catalog no. L2254). PCR primers were from Operon (Huntsville, AL).

5.2.4. Cell Culture and lipid treatments—Human Brain Microvascular Endothelial Cells (HBMEC) (ACBRI 376) (passage 6, Cell Systems Corp., Kirkland, WA) were cultured in CSC Complete Serum-Free Medium (SF-4Z0-500) and CSC Complete Medium which includes 10% serum (4Z0-500); CSC Attachment Factor™ (4Z0-210) under an atmosphere of 5 % CO_2: 95% air and 37°C. Cells were exposed for 3 hr to the following conditions, media, TGRL (T) (150 mg/dL =1.5 mg/mL), Lipoprotein lipase (L) (2U/mL), and T (150 mg/dL) + L (2U/mL) pre-incubated for 30 minute at 37°C before application. Cells treated with T + L are referred as "lipolysis" from here on. To test the suppression of compounds, cells were pre-treated with the 200 μM of the indicated compound for 30 min.

5.2.5. mRNA expression by quantitative RT-PCR (qRT-PCR)—RT-PCR was performed to evaluate the TGRL lipolysis induced gene expression. After incubation cells were washed with cold PBS and total RNA was extracted from Control and treated 6-well plate using RNeasy Mini Kit (Qiagen, Valencia, CA) including the DNA digestion step as described by the manufacturer. A 5 μg of total RNA extracted from each sample was reverse-transcribed to obtain cDNA using Superscript-III reverse transcriptase kit (Invitrogen, Carlsbad, CA) as described by the manufacturer. The real-time polymerase chain reaction (RT-PCR) method with SYBR Green as fluorescent reporter was used to quantify the gene expression. The gene specific primers were designed with Primer Express 1.0 software (Applied Biosystems) using designed from published cDNA sequences as follows: ATF3 (GenBank acc. no. NM_001674): 5'-TTCTCCCAGCGTTAACACAAAA-3' (forward) and 5'-AGAGGACCTGCCATCATGCT-3' (reverse); IL-8 (GenBank acc. no. NM_000584): 5'- CCTTTCCACCCCAAATTTATCA-3' (forward) and 5'- TGGTCCACTCTCAATCACTCTCAG -3' (reverse); PTGS2 (also known as COX-2) (GenBank acc. no. NM_000963): 5'- CTGAATGTGCCATAAGACTGACCT-3' (forward) and 5'- TCCACAGATCCCTCAAAACATTT-3' (reverse). The reaction was carried out in 384 well optical plates containing 25 ng RNA in each well. The applied RNA quantity was normalized by amplifying cDNA samples simultaneously with glyceraldehyde-3-phosphate dehydrogenase (GAPDH) specific primers: 5'-CACCAACTGCTTAG-3' (forward) and 5'- TGGTCATGAGTCCT-3' (reverse). The transcript levels were measured by real-time RT-PCR using the ABI PRISM 7700 Sequence detection system (PE Applied Biosystems, Foster City, CA). The PCR amplification parameters were: initial denaturation step at 95°C for 10 min followed by 40 cycles, each at 95°C for 15 s (melting) and 60°C for 1 min (annealing and extension). A comparative C_T method [29] was used to calculate relative changes in gene expression determined from real-time quantitative PCR experiments

(Applied Biosystems User Bulletin No.2 (P/N4303859). The threshold cycle, C_t, which correlates inversely with the target mRNA levels, was measured as the cycle number at which the SYBR Green emission increases above a preset threshold level. The specific mRNA transcripts were expressed as fold difference in the expression of the specific mRNAs in RNA samples from the TGRL lipolysis treated cells compared to those from the TGRL alone treated cells.

Acknowledgments

References

1. (a) Roetne-Jakob R, Jacobsen H. Alzheimer's Disease: From Pathology to Therapeutic Approaches. Angewandte Chemie. 2009; 48:3030–3059. [PubMed: 19330877] (b) Mattson MP. Pathways towards and away from Alzheimer's disease. Nature. 2004; 430:631–639. [PubMed: 15295589]

2. Kabalka GW, Namboodiri V, Akula MR. Synthesis of 123I labeled Congo Red via solid phase organic chemistry. J. Labeled Cpd. Radiopharm. 2001:921–929.

3. Klunk WE, Wang J, Huang G-F, Debnath ML, Holt DP, Mathis CA. Uncharged thioflavin-T deribatives bind to amyloid-beta protein with high affinity and readily enter the brain. Life Sci. 2001:1471–1484. [PubMed: 11554609]

4. Lee WC, Kung MP, Hou C, Kung HF. Dimethylamino-fluorenes: ligands for detecting β-amilod plaques in the brain. Nucl. Med. Biol. 2003; 30:573–580. [PubMed: 12900283]

5. Riviére C, Richard T, Quentin L, Krisa S, Mérillon J-M, Monti J-P. Inhibitory activity ofstilbenes on Allzheimer's β-amyloid fibrils in vitro. Bioorg. Med. Chem. 2007; 15:1160–1167. [PubMed: 17049256]

6. Torok M, Milton S, Kayed R, Wu P, McIntire T, Glabe CG, Langen R. Structural and dynamic features of Alzheimer's Abeta peptide in amyloid fibrils studied by site-directed spin labeling. J Biol. Chem. 2002; 277:40810–40815. [PubMed: 12181315]

7. Wu J, Breydo L, Isas JM, Lee J, Kuznetsov ZG, Langen R, Glabe C. Fibrillar Oligomers Nucleate the Oligomerization of Monomeric Amyloid beta but Do Not Seed Fibril Formation. J. Biol. Chem. 2009; 285:6071–6079. [PubMed: 20018889]

8. Esposito C, Tedeschi A, Scrima M, D'Ericcdo G, Ottaviani MF, Rovero P, D'Ursi AM. Exploring interaction of beta-amyloid segment (25-35) with membrane models through paramagnetic probes. J. Peptide Sci. 2006; 12:766–774. [PubMed: 17131288]

9. Zubenko GS, Kopp U, Seto T, Firestone TLL. Platelet membrane fluidity individuals at risk for Alzheimer's disease: a comparison of results from fluorescence spectroscopy and electron spin resonance spectroscopy. Psychopharmacology. 1999; 145:175–180. [PubMed: 10463318]

10. Lin MT, Beal MMF. Mitochondrial dysfunction and oxidative stress in neurodegenerative diseases. Nature. 2006; 443:787–795. [PubMed: 17051205]

11. Lipton SA. Paradigm shift in neuroprotection by NMDA receptor blockade: memantine and beyond. Nat. Rev. Drug Discov. 2006; 5:160–170. [PubMed: 16424917]

12. Lam AM, Pattison DI, Bottle SE, Keddie JD, Davies JM. Nitric Oxide and Nitroxides Can Act as Efficient Scavengers of Protein –Derived Free Radicals. Chem. Res. Toxicol. 2008; 21:2111–2119. [PubMed: 18834151]

13. Krishna MC, Russo A, Mitchell JB, Goldstein S, Hafni H, Samuni A. Do nitroxide antioxidants act as scavengers of O2.-or as SOD mimics? J. Biol. Chem. 1996; 271:26026–26031. [PubMed: 8824242]

14. Glebska J, Pulaski L, Gwozdzinski K, Kolimowski J. Structure-activity relationship studies of protective function of nitroxides in Fenton system. BioMetals. 2001; 14:159–170. [PubMed: 11508849]

15. Twomey P, Taira J, DeGraff W, Mitchell JB, Russo A, Krishna MC, Hankovszky HO, Frank L, Hideg K. Direct Evidence for In Vivo Nitroxide Free Radical Production from a New Antiarrhythmic Drug by EPR Spectroscopy. Free Rad. Biol. Med. 1997; 22:909–916. [PubMed: 9119261]

16. Bobko A, Kirilyuk IA, Grigor'ev IA, Zweier JL, Khramtsov VV. Reversible reduction of nitroxides to Hydroxilamines: Roles of ascorbate and glutathione. Free Rad. Biol. Med. 2007; 42:404–412. [PubMed: 17210453]

17. Dikalov SI, Vitek MP, Maples KR, Mason RP. Amiloid β Peptides Do not Form Peptide-derived Free Radicals Spontaneously, but Can Enhance Metal-catalyzed Oxidation of Hydroxylamines to Nitroxides. J. Biol. Chem. 1999; 274:9392–9399. [PubMed: 10092619]

18. Butterfield AD, Martin L, Carney JM, Hensley K. Aβ(25-35) Peptide Displays H2O2-like reactivity towards aqueous Fe^{2+}, nitroxide spin probes, and synaptosomal membrane-proteins. Life Sci. 1995; 58:217–228. [PubMed: 9499162]

19. Prasad KN, Hovland AR, Cole WC, Prasad KC, Nahreini P, Prasad-Edwards J, Andreatta CP. Multiple Antioxidants int he Prevention and treatment of Alzheimer Disease: Analysis of Biologic Rationale. Clin. Neuropharm. 2000; 23:2–13.

20. Hankovszky HO, Hideg K, Lex L, Nitroxyls L. VII. Synthesis and Reactions of Highly Reactive 1-Oxyl-2,2,5,5-tetramethyl-2,5-dihydropyrrole-3-ylmethyl Sulfonates. Synthesis. 1980:914–916.

21. Csek J, Hankovszky HO, Hideg K. Synthesis of novel, highly reactive 1-oxyl-2,2,6,6-tetramethyl-1,2,3,6-tetrahydropyridine derivatives. Can. J. Chem. 1985; 63:940–943.

22. Kálai T, Balog M, Jek J, Hideg K. 3-Substituted-2,2,5,5-tetramethyl-2,5-dihydro-1H-pyrrol-1-yloxyl Radicals as a Verstile Synthon for Synthesis of New Paramagnetic Heterocycles. Synthesis. 1998:1476–1482.

23. Columbus L, Kálai T, Jek J, Hideg K, Hubbell WL. Molecular Motion of Spin Labeled Side Chains in alpha-Helices: Analysis by Variation of Side Chain Structure. Biochemistry. 2001; 40:3828–3846. [PubMed: 11300763]

24. Sár PC, Kálai T, Bárácz MN, Jerkovich G, Hideg K. Selective Reduction of Nitrones and Nitroxides to Functionalized Secondary Amines. Synthetic Commun. 1995; 25:2929–2940.

25. Bognár B, Ahmed S, Kuppusamy ML, Selvendrian K, Khan M, Jek MJ, Hankovszky HO, Kálai T, Kuppusamy P, Hideg K. Synthesis and study of new paramagnetic and diamagnetic verapamil derivatives. Bioorg. Med. Chem. 2010; 18:2954–2963. [PubMed: 20347319]

26. Hong HS, Maezawa I, Budamagunta M, Rana S, Shi A, Vassar R, Liu R, Lam KS, Cheng RH, Hua DH, Voss JC, Jin L-W. Candidate anti-Aβ fluorene compounds selected from analogs of amyloid imaging agents. Neurobiol Aging. (in press).

27. Khan NC, Wilmot M, Rosen GM, Demidenko E, Sun J, Joseph J, O'Hara J, Kalyanaraman B. H. M. Spin traps: in vitro toxicity and stability of radical adducts. Free Rad. Biol. Med. 2003; 34:1473–1481. [PubMed: 12757857]

28. Glass CK, Saijo K, Winner B, Marchetto MC, Cage FH. Mechanisms underlying inflammation in neurodegeneration. Cell. 2010; 140:918–34. [PubMed: 20303880]

29. Livak KJ, Schmittgen TD. Analysis of relative gene expression data using real-time quantitative PCR and the 2(-Delta Delta C(T)) Method. Methods. 2001; 25:402–408. [PubMed: 11846609]
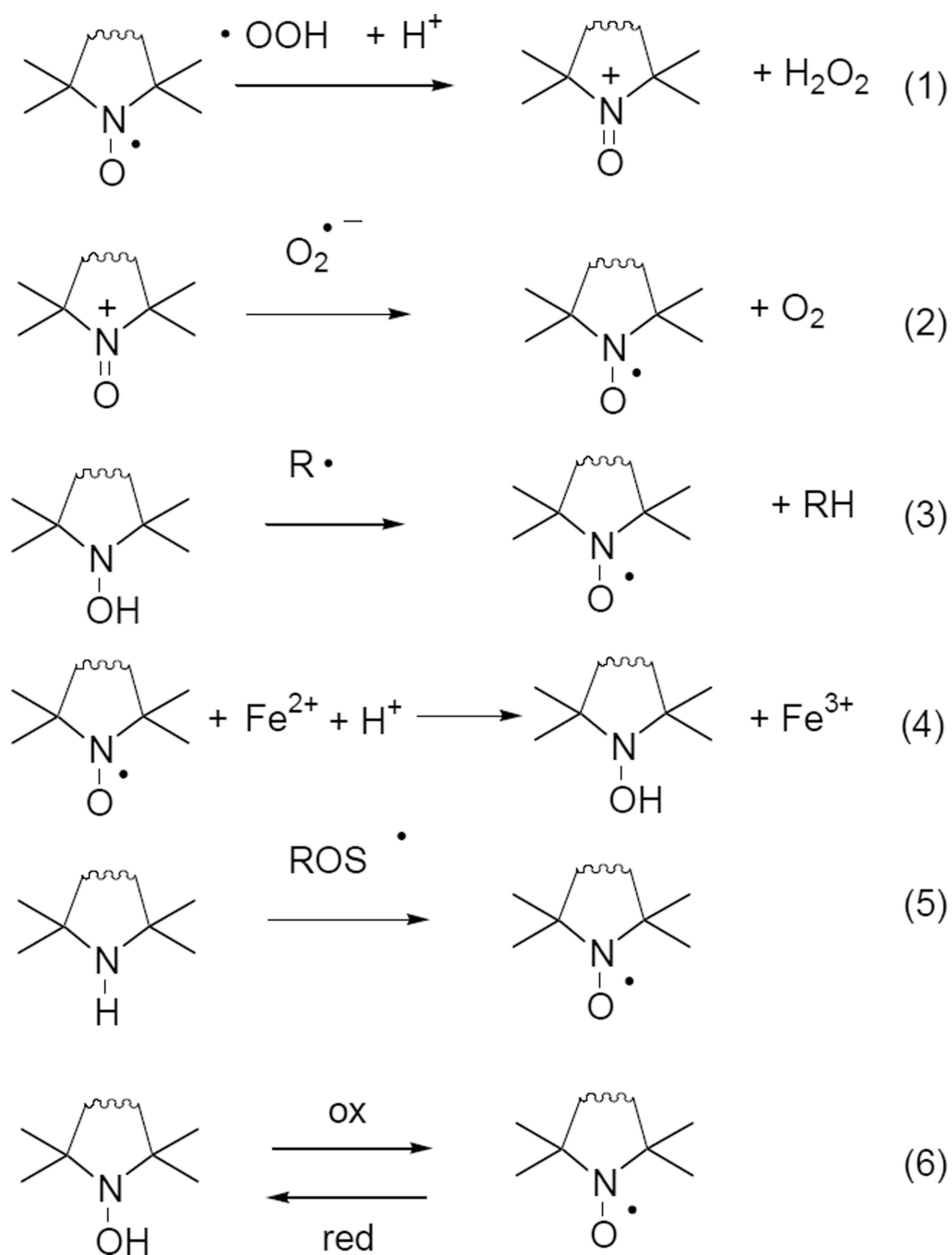
$$\cdot OOH \ + \ H^+ \ \longrightarrow \ + \ H_2O_2 \quad (1)$$

$$O_2^{\cdot -} \ \longrightarrow \ + \ O_2 \quad (2)$$

$$R\cdot \ \longrightarrow \ + \ RH \quad (3)$$

$$+ \ Fe^{2+} + \ H^+ \ \longrightarrow \ + \ Fe^{3+} \quad (4)$$

$$ROS^{\cdot} \ \longrightarrow \quad (5)$$

$$\underset{red}{\overset{ox}{\rightleftarrows}} \quad (6)$$

Figure 1.
Possible radical scavenging mechanisms and transformations of nitroxides and pre-nitroxides.
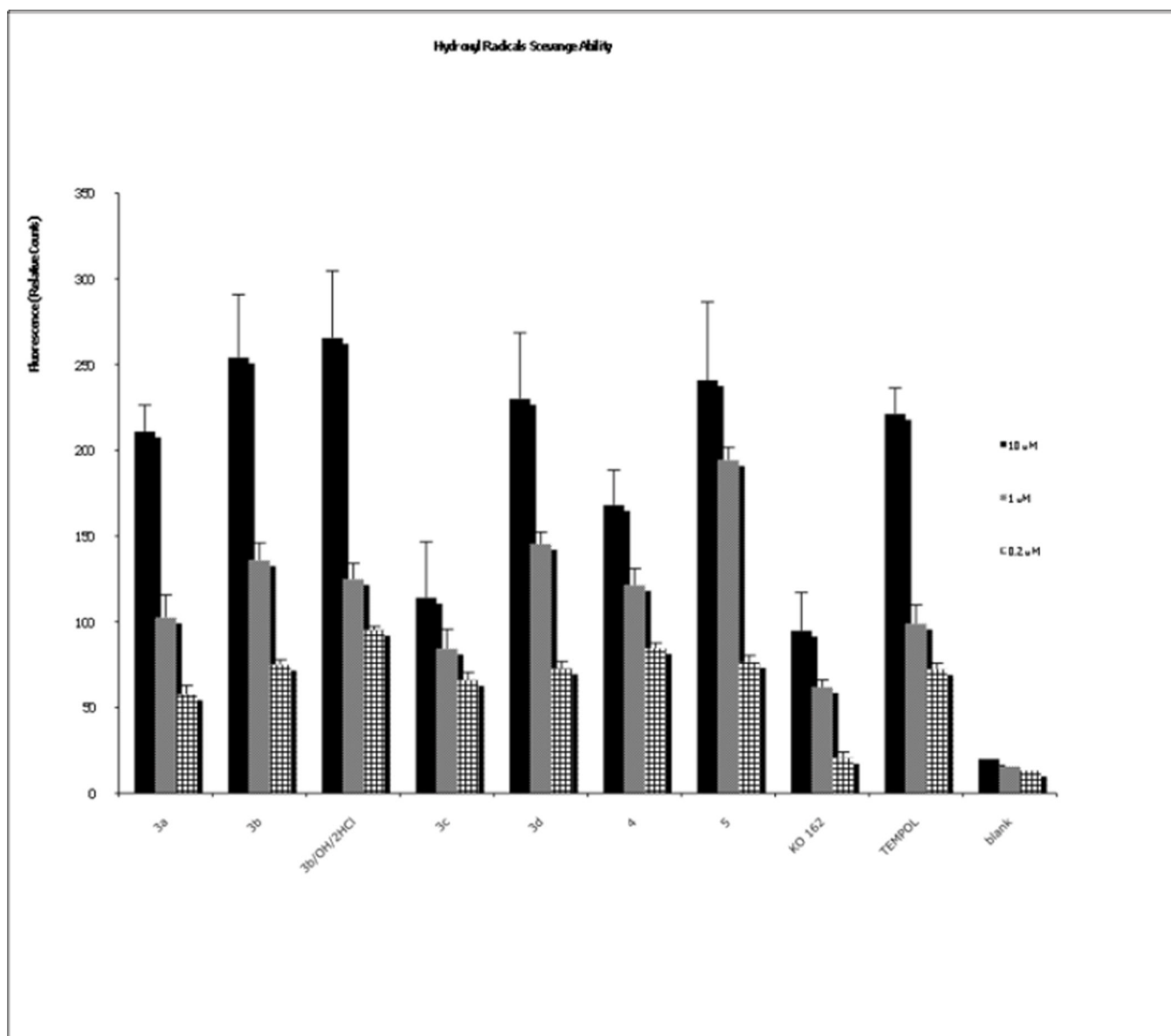
Figure 2.
Hydroxyl radical scavenging ability of compounds **3–5 by** HORAC assay. As a control samples were used distilled water.
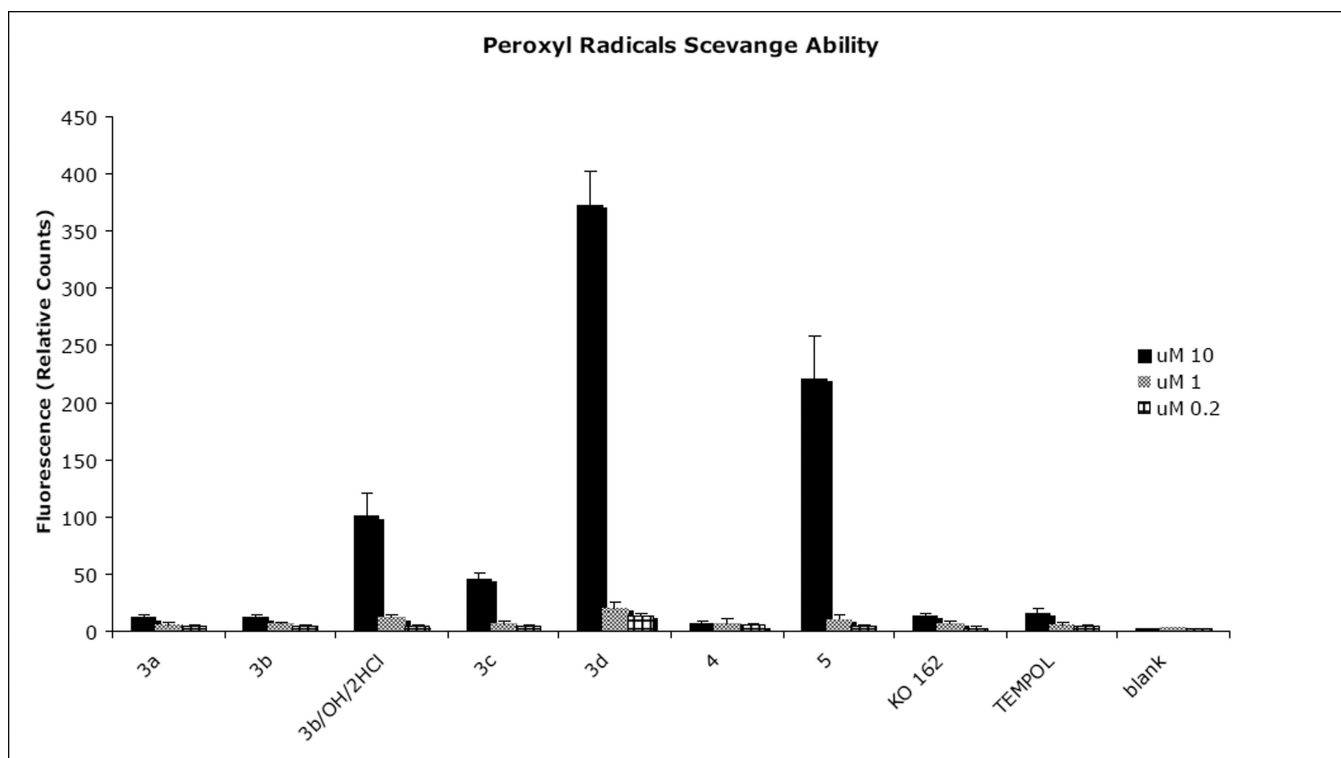
Figure 3.
Peroxyl radical scavenging ability of compounds **3–5 by** ORAC assay. As a control samples were used distilled water.
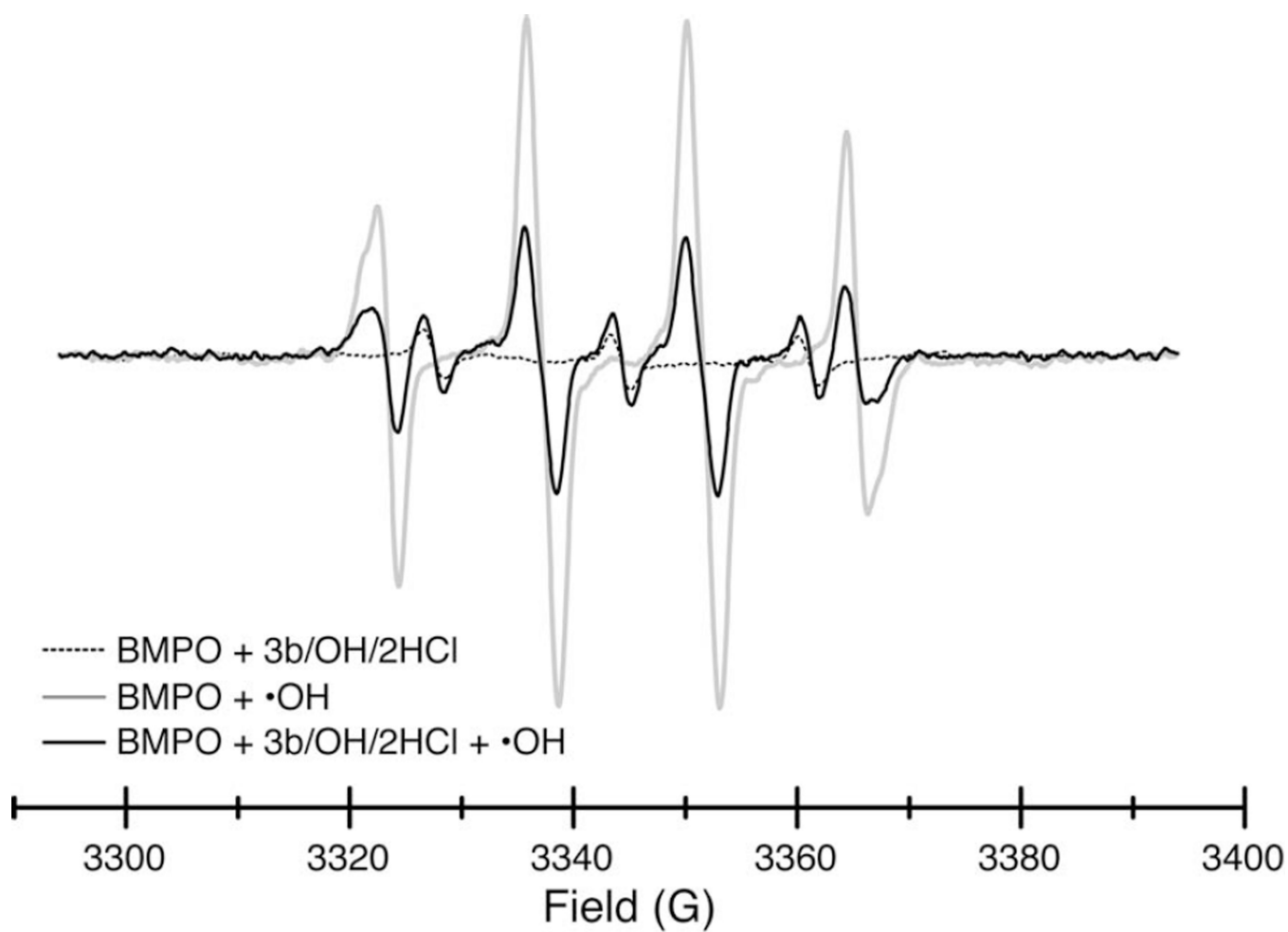
Figure 4.
EPR scans in the presence of the BMPO spin trap of compound **3b/OH/2HCl** (dotted), the BMPO-•OH adduct (grey), and the BMPO-•OH adduct in the presence of **3b/OH/2HCl** (black). See text for experimental details.
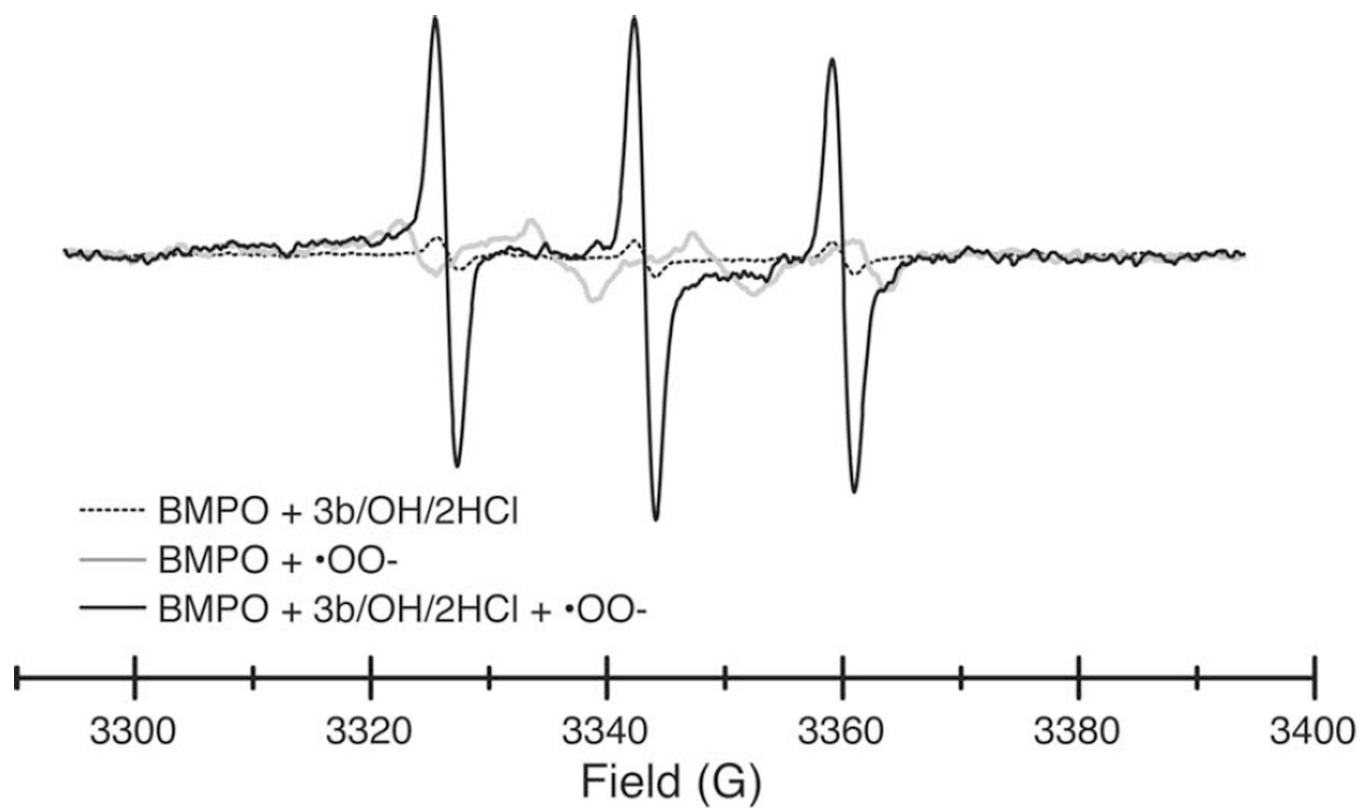
Figure 5.
EPR scans in the presence of the BMPO spin trap of compound **3b/OH/2HCl** (dotted), the BMPO-OO• adduct (grey), and the BMPO-OO• adduct in the presence of **3b/OH/2HCl** (black). See text for experimental details.
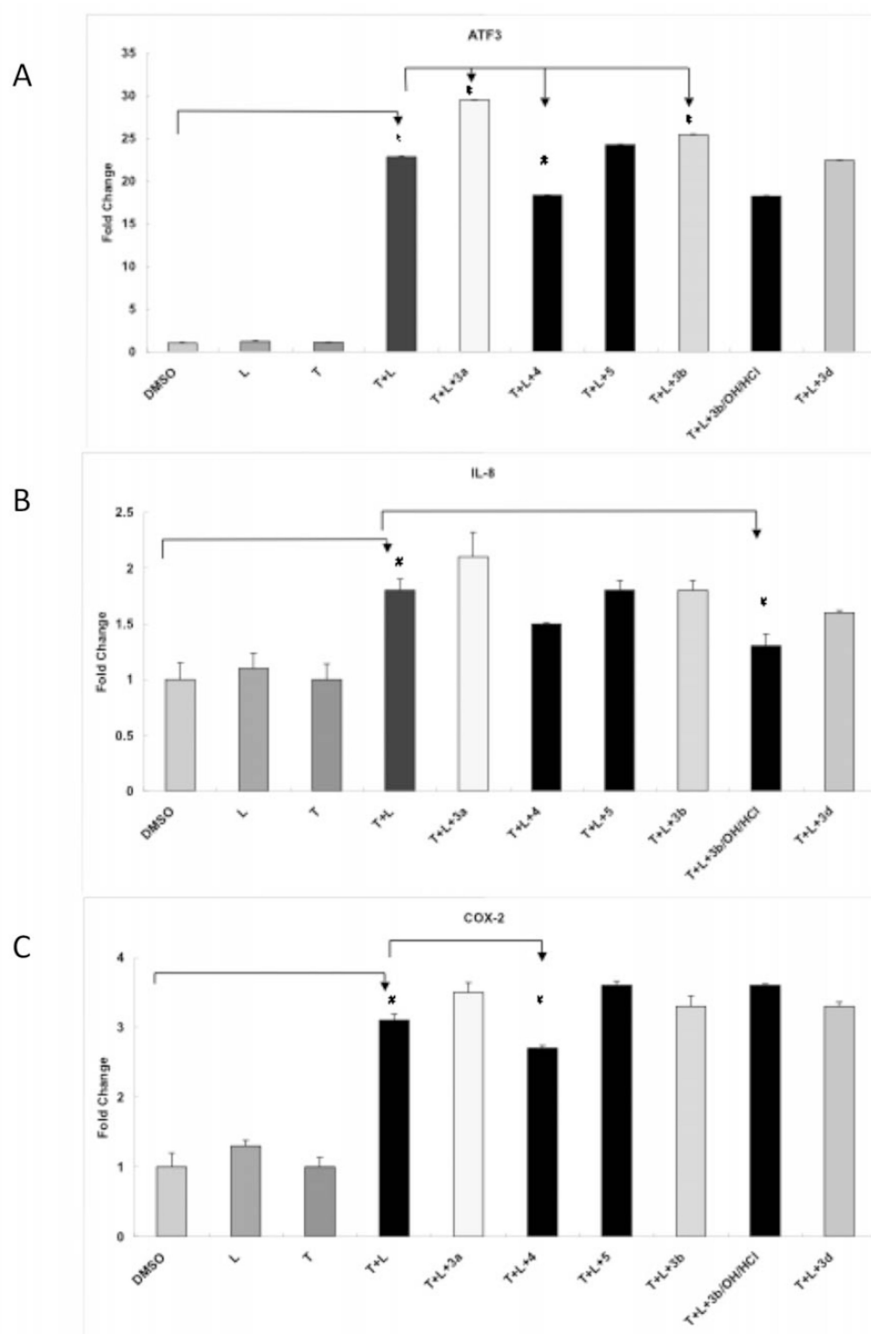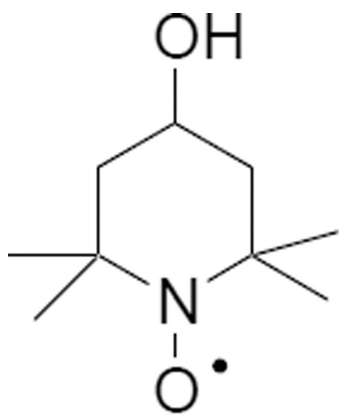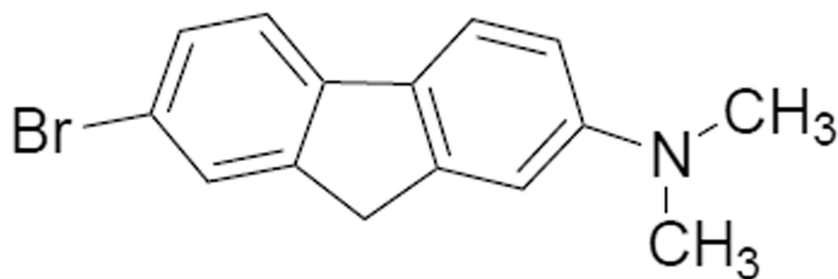
Figure 6.
TGRL lipolysis products induced gene expression was suppressed by compounds in HBMVEC. A) mRNA expression of activating transcription factor (ATF3) was significantly suppressed by compounds 4 and further induced by compounds 3a and 5 compared to TGRL lipolysis products treated cells. B) mRNA expression of interleukin 8 (IL-8) was significantly suppressed by compounds 3b compared to TGRL lipolysis products treated cells. C) mRNA expression of cyclooxygenase 2 (COX-2) was significantly suppressed by compounds 4 compared to TGRL lipolysis products treated cells. N = 3, * = P 0.002 and # = P 0.05. T = Triglyceride-rich lipoproteins, L = lipoprotein lipase.

Scheme 1.
(a) **2a-d** (1.0 equiv.), K$_2$CO$_3$ (1.0 equiv.), DMSO, 60 °C, 6 h, 38–45%; (b) (H$_2$CO)$_n$ excess, NaBH$_3$CN (6.0 equiv.), AcOH, rt., 18h, then PbO$_2$, O$_2$, 15 min., 64%; (c) Fe (10.0 equiv.), AcOH, 70 °C, 30 min., 47%; (d) EtOH/HCl, rt., 15 min. 71%.

TEMPOL

KO-162

Scheme 2.
Chemical structure of TEMPOL and KO-162.

Table 1

Hydroxyl and peroxyl radical scavenging ability of compounds **3a-d, 4, 5** estimated by integration of EPR band area

Compound	Hydroxyl radical scavenging ability (%)[*] by EPR	Peroxyl radical scavenging ability (%) by EPR
3a (HO-4160)	28	73
3b (HO-4191)	26	ND
3b/OH/2HCl (HO-4191/OH/2HCl)	61	80
3c (HO-4192)	10	ND
3d (HO-4198)	29	100
4 (HO-4161)	18	ND
5 (HO-4166)	18	100

[*] Based on 3 measuments, accuracy ± 5%. ND: not determined.